ORIGINAL PAPER

Simultaneous voltammetric detection of dopamine and uric acid in the presence of high concentration of ascorbic acid using multi-walled carbon nanotubes with methylene blue composite film-modified electrode

Suling Yang · Gang Li · Ran Yang · Miaomiao Xia · Lingbo Qu

Abstract An electrochemically functional nanocomposite through the adsorption of methylene blue onto the multi-walled nanotubes (MB-MWNTs) was prepared, and a sensitive voltammetric sensor was fabricated. The modified electrode showed excellent electrocatalytic activity toward dopamine (DA) and uric acid (UA) in 0.1 M phosphate solution medium (pH 3.0). Compared to the bare electrode, the MB-MWNTs film-modified electrode not only remarkably enhanced the anodic peak currents of DA and UA, i.e., shifted the anodic peak potential of DA negatively, but also avoided the over-lapping of the anodic peaks of DA and UA. The interference of ascorbic acid (AA) was eliminated. Under the optimized conditions, the peak separation between AA and DA and between DA and UA was 219 and 174 mV, respectively. In the presence of 1.0 mM AA and 10.0 μM UA, the anodic peak current was linear to the concentration of DA in the range of 0.4–10.0 μM with a detection limit of 0.2 μM DA. The anodic peak current of UA was linear to the concentration in the range of 2.0–20.0 and 20.0–200.0 μM with a lowest detection limit of 1.0 μM in the presence of 1.0 mM AA and 1.0 μM DA.

Keywords Electrocatalytic · Dopamine · Uric acid · Multi-walled carbon nanotube · Methylene blue

S. Yang · R. Yang · M. Xia · L. Qu (✉)
Department of Chemistry, Zhengzhou University,
Zhengzhou 450001, People's Republic of China
e-mail: qulingbu@zzu.edu.cn

S. Yang
e-mail: yang_suling@163.com

G. Li · L. Qu
College of Chemistry and Chemical Engineering,
Anyang Normal University,
Anyang 455002, People's Republic of China

L. Qu
Chemistry and Chemical Engineering School,
Henan University of Technology,
Zhengzhou 450001, People's Republic of China

Introduction

Dopamine (DA), as one of the most important catechol-amines, is a significant neurotransmitter and plays a vital role in the central nervous, renal, hormonal, and cardiovascular systems [1, 2]. Inadequate DA-containing neurons may cause neurological disorders such as schizophrenia and Parkinson's disease [3]. Therefore, determining the concentration of this neurochemical is of great clinical importance. Uric acid (UA) is one of the principal end-products of purine metabolism in the human body. Abnormal levels of UA are symptoms of several diseases like gout, hyperuricaemia and Lesch–Nyhan syndrome [4]. Hence, monitoring the concentration of UA in biological fluids has their clinical significance. Electrochemical methods can be used to determine DA and UA due to their electrochemical active. But the significant problem was encountered with the detection of DA or UA using electrochemical methods arising from the primary interference of ascorbic acid (AA). Generally, AA, DA, and UA always coexist in biological fluids, and AA has an overlapping oxidation peak of DA and UA at bare electrodes, which results in poor selectivity determination of DA or UA in real samples. Therefore, it is essential to eliminate the interference of AA by using a suitable film-modified electrode for the selective determination of DA and UA. For this purpose, various modified

electrodes have been developed. For example, DA and UA can be selectively detected in the presence of AA at electrodes modified with poly(acrylic acid) multi-walled carbon nanotubes (MWCNTs) [5], deoxyribonucleic acid (DNA)/poly(p-aminobenzensulfonic acid) bilayer [6], RNA film [7], functionalized single-walled carbon nanotube (SWCNT) [8], LaFeO$_3$ [9], single-walled carbon nanohorn [10], poly(eriochrome black T) [11], functionalized thiadiazole [12], CDDA film [13], poly(acid chrome blue K) [14], poly(vinyl alcohol) [15], oracet blue (OB) [16], mesoporous carbon/Nafion [17], etc. Although the voltammetric techniques focusing on the high selective, low costly, and little time-consuming simultaneous determination of DA and UA with various modified electrodes have already been reported, it is still significant to exploit more economical, efficient, and convenient voltammetry for simultaneous determination of DA and UA.

In recent years, carbon nanotubes (CNTs) have received more and more attention to the electrode preparation. Since being discovered by Lijima in 1991 [18], CNTs have obtained increasing applications in chemical, physical and material fields owing to their unique structure and extraordinary properties. CNTs have excellent electronic properties, such as huge surface area and efficient catalytic activity, which suggest that they can promote charge transfer reaction when they are employed as electrode materials [19, 20].

Methylene blue (MB), as an electroactive conjugated cationic dye, is always used as a redox indicator because its formal potential is between 0.08 and −0.25 V (vs. SCE) in solution with pH 2–8 [21]. The combination of MB and the bare electrode is relatively weak due to the low molecular weight of MB, and MB is subjected to loss from the mass of absorbed MB molecule on the electrode surface. In order to overcome this problem, great efforts have been devoted to load MB using electrodes modified with nanomaterials such as nano-Cu$_2$O [22], nano-SiO$_2$ [23], and nano-TiO$_2$ [24]. Yan and co-workers [25] described the adsorption of electroactive MB dye onto SWCNTs to form an electrochemically functional nanostructure. Yogeswaran and Chen [26] deposited MB by the electrochemical oxidation of MB on the MWCNTs modified electrodes for electroanalytical of catecholamine and AA. To the best of our knowledge, the present strategy for the preparation of an electrochemically functional nanocomposite through the adsorption of MB onto the MWNTs (MB-MWNTs) as the modifier for simultaneous voltammetric detection of DA and UA in the presence of high concentration of AA has not been reported so far.

CNTs are provided with a π-conjugative structure and a highly hydrophobic surface. This unique property of the CNTs can allow some organic conjugated compounds to interact with sidewalls of CNTs through π–π electronic and hydrophobic interactions to form new composite materials [27, 28]. Layer-by-layer assembled CNTs adsorbed by polymer have been developed for the electrocatalytic detection of DA in the presence of AA [29]. Some sandwiched films also were applied to the designing of nanodevices with the help of noncovalent adsorption, electrodeposition, and so on [30].

In this report, we prepared an electrochemically functional nanocomposite through the adsorption of MB-MWNTs and fabricated a sensitive voltammetric sensor using the functional nanocomposite for the simultaneous detection of DA and UA in the presence of AA. The MB-MWNTs nanocomposite showed the advantages of carbon nanotube with a high surface area and good affinity of MB for DA and UA contraction. Well-defined redox peaks of DA appeared after modification of MB-MWNTs. DA, uric acid and AA can be well separation on the modified electrode. The composite film-modified electrode showed remarkable selectivity and high sensitivity for DA and uric acid, and eliminate interference from high concentration AA. Thus, the modified electrode could simultaneously detect DA and UA in the presence of high concentrations of AA.

Experimental

Reagents and chemicals

DA, UA, and AA were purchased from Alfa Aesar China (Tianjin) Co., Ltd. and used as received. The MWCNTs (diameter: 10–20 nm, length: 1 to 2 μm, purity >95%) were obtained from Shenzhen Nanotech Port Co., Ltd., China. Nafion (wt. 5%) and MB was purchased from Sigma. All the other chemicals used were analytical grade without further purification and prepared with double distilled water. pH of the solutions was adjusted with 0.1 M H$_3$PO$_4$. Solutions were deoxygenated by purging with pre-purified nitrogen gas.

Apparatus

RST3000 electrochemical system (Suzhou Risetech Instrument Co., Ltd., Suzhou, China) was employed for all the voltammetric measurement. A conventional three-electrode system was used including a bare glassy carbon electrode (GCE) (d=4 mm) or MB-MWNTs film-modified GCE as working electrode, a saturated calomel electrode (SCE) as reference electrode, and a platinum wire electrode as auxiliary electrode. All the pH values were measured with a PHS-3C precision pH meter (Leici Devices Factory of Shanghai, China), which was calibrated with standard buffer solution every day. The scanning electron microscopy (SEM) was performed with JEOL-

JSM-6700F field emission scanning electron microscope (Japan). The ultraviolet–visible (UV–vis) spectra were recorded with a Model UV-2102PC spectrophotometer (UNICO, Shanghai, China). A Model 5500 atomic force microscope (AFM, Agilent, USA) was used to study the morphology of the MWNTs and MB-MWNTs power samples.

Preparation of MB-MWNTs composite film-modified GCE

The bare GCE was pretreated carefully with 0.05 μm alumina slurry on a polishing cloth, rinsed thoroughly with 1:1 HNO_3–H_2O (v/v), and then washed with pure ethanol and redistilled water, respectively. Untreated MWNTs (1.0 g) was added to plentiful concentrated nitric acid (wt. 68%) and then sonicated for about 4 h. The mixture was filtrated and washed with doubly distilled water until the filtrate was litmusless. The treated MWNTs were dried under an infrared lamp. 16.0 mg treated MWNTs were dispersed in 5.0 ml 1.0×10^{-4} M MB aqueous solution and sonicated for an hour. When the mixture was filtrated, the blue color of MB solution became lighter, which indicated that MB had already absorbed on the MWNTs. The mixture was washed with enough doubly distilled water to remove the weak absorbed MB. MB-MWNTs suspension was accomplished as follows: Above MB-MWNTs, composite 5.0 mg was sonicated in 5.0 ml Nafion (wt. 0.1%) methanol solution for about 30 min and then homogeneous suspension would be achieved. The pretreated GCE was coated evenly with 10.0 μl of MB-MWNTs suspension, and then methanol was evaporated at room temperature. So MB-MWNTs/GCE was achieved. For contrast, MWNTs/GCE, MB/GCE was prepared with the same procedure without MB or MWNTs.

Analytical procedures

Except as otherwise stated, 0. 1 M NaH_2PO_4–H_3PO_4 buffer solution (pH 3.0) was used as supporting electrolyte for the determination of DA and UA. Voltammograms were obtained by scanning the potential from −100 to 900 mV (vs. SCE). The quantitative determinations of DA and UA were achieved by measuring the oxidation peak currents after background subtraction using differential pulse anodic stripping voltammetry (DPASV). In order to fit into the linear range of the method, the urine sample employed for operation was accurately diluted by a factor of 1/100 (v/v) with the supporting electrolyte, DA hydrochloride injection (standard concentration of DA 10 mg/ml, 2 ml per injection) by a factor of 1/10000 (v/v). The dilution process can actually help reducing the matrix effect of real samples.

Results and discussion

Spectral and electrochemical evidence for MB adsorption onto MWNTs

In order to ascertain the formation of MB-MWNTs nanostructure, UV–vis spectral measurements were carried out. As shown in Fig. 1, the absorption spectra of water-dispersed solutions of free MB (curve a), MWNTs (curve b) and the MB-MWNTs adduct (curve c) were displayed. The UV–vis spectrum of the MWNTs dispersed in aqueous solution exhibited a strong absorbance at 263 nm. The spectrum of free MB in aqueous solution displayed two strong absorption peaks at 294 and 665 nm (curve a), characteristic of the MB monomer in solution. The chemisorption of MB-MWNTs was evident from the spectrum of the MB-MWNTs composite (curve c), which was similar to that of MWNTs. However, a close inspection of the spectrum of MWNTs and the MB-MWNTs adsorptive nanostructure revealed that there was a change in the spectrum of MWNTs after its adsorption of MB. A new peak appeared at 690 nm was observed, which was due to the absorbance of the aggregation of MB molecules onto the MWNTs [31].

Figure 2 presented the morphology of MWNTs (Fig. 2a, b) and MB-MWNTs (Fig. 2c, d) powder samples on a mica sheet, obtained by an AFM. The powder samples showed the existence of MWNTs in a network-like structure with an unorderly arrangement. The adsorption of MB on MWNTs seemed to break the intertwist into individual CNTs. In addition, some breaking and shortening of MWNTs into smaller ones were obvious. The average diameter of individual strand of MWNTs was about 38.05 nm. The average diameter of individual strand
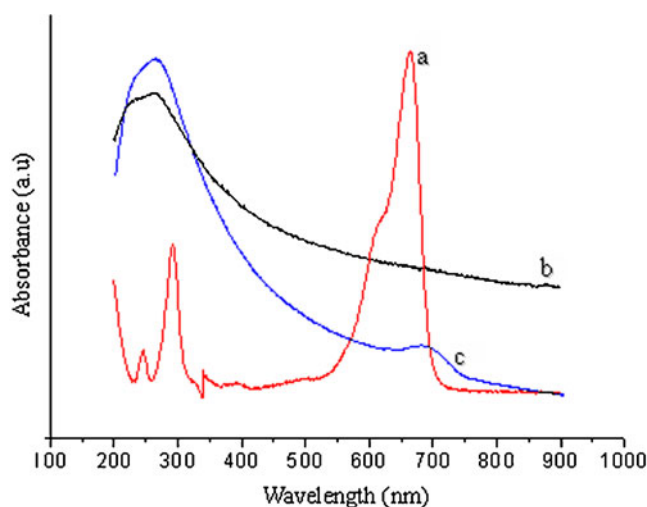
Fig. 1 Absorption spectrum of aqueous dispersion of MB (*a*), aqueous dispersion of MWNTs (*b*), and aqueous dispersion of MB-MWNTs (*c*)
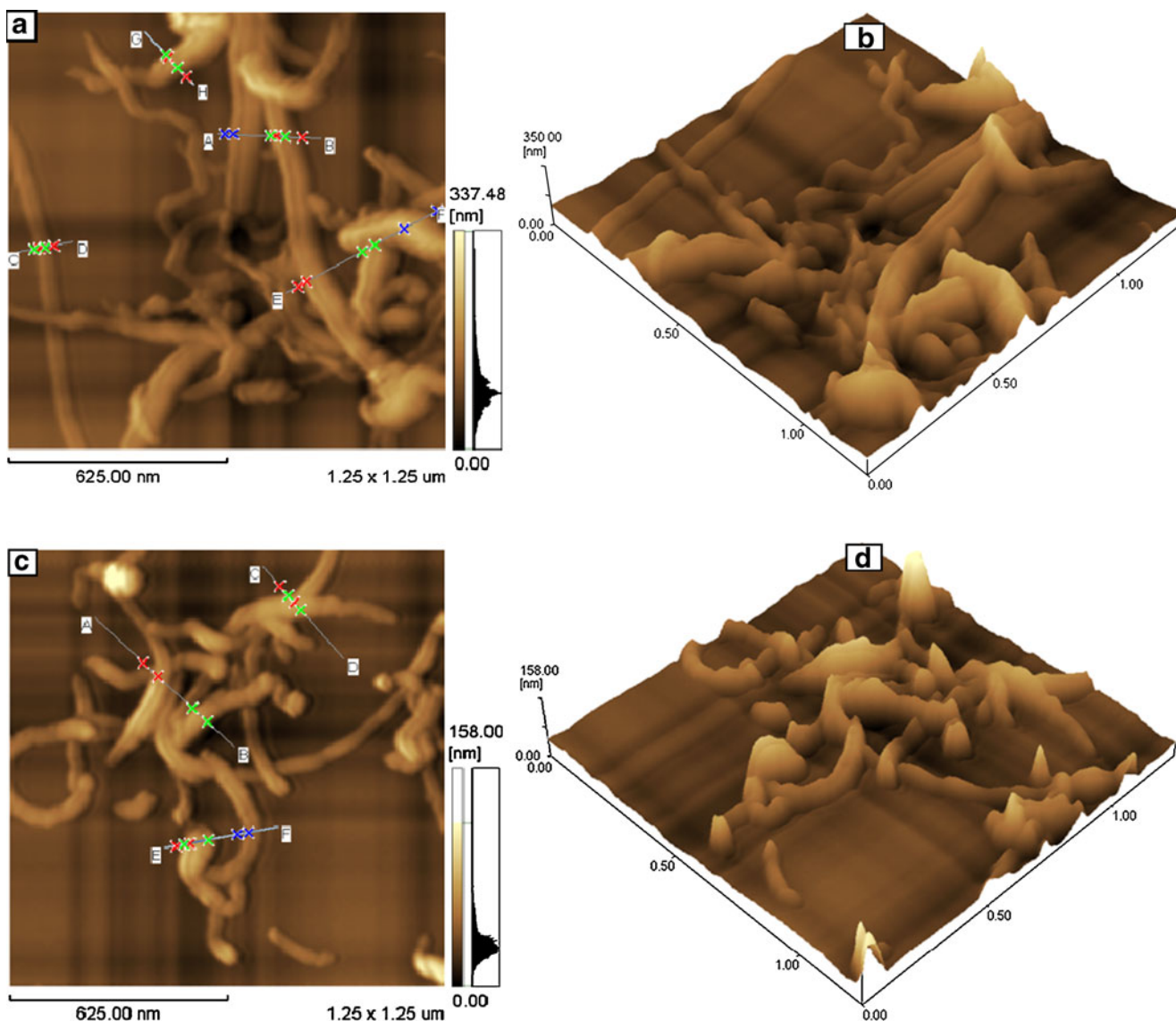
Fig. 2 AFM image of MWNTs (**a**, **b**) and MB-MWNTs (**c**, **d**) power samples on a mica sheet

of MB-MWNTs was about 62.03 nm, which was nearly twice that of MWNTs indicating clearly that the individual strand of MWNTs was entirely encapsulated or wrapped by the MB to form a tubular composite. Moreover, the MB-MWNTs sample could be readily dispersed in water to give a black-colored solution, but the MWNTs couldn't be easily dissolved or dispersed in aqueous solution. This observation again indicated an adsorption of MB on MWNTs.

Figure 3 demonstrated cyclic voltammograms of the MWNTs/GCE (curve a) and MB-MWNTs/GCE (curve b) immersed into 0.1 M pure phosphate buffer (pH 3.0) containing no MB. There was no any redox wave of MWNTs/GCE in the potential range of −400 to 600 mV. In contrast to MWNTs/GCE, a pair of redox waves of the MB-MWNTs/GCE was observed at 95 and 27 mV, suggesting

that electroactive MB can adsorb onto the MWNTs and form an electrochemically functional nanostructure.

Figure 4 showed the results of the electrochemical impedance spectra (EIS) of a bare GCE, MWNTs/GCE and MB-MWNTs/GC electrode in a solution containing 0.1 M KCl and 1.0 mM $Fe(CN)_6^{3-/4-}$. The Nyquist plot exhibited a poor small semicircle portion at higher frequencies, and a line at lower frequencies for the bare GCE (Fig. 4a), which was similar to the characteristic of a diffusion limiting step of the electrochemical process. However, at MWNTs/GCE, the Nyquist plots displayed a clear bigger semicircular feature in addition to the linear feature (Fig. 4ba). The semicircle portion, as observed at higher frequencies, was associated with a process that was limited by electron transfer. The linear features observed at lower frequencies were attributed to diffusion-limited
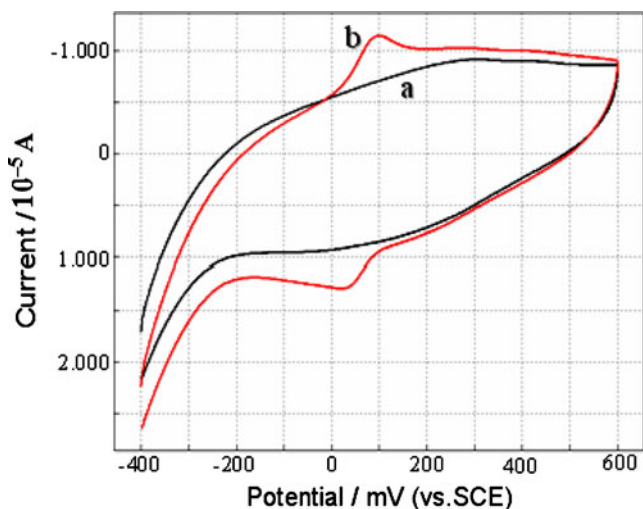
Fig. 3 Cyclic voltammograms of the MWNTs/GCE (*a*) and MB-MWNTs/GCE (*b*) in 0.1 M phosphate buffer (pH 3.0); scan rate 80 mV/s

electron transfer. Adsorption of MB on the MWNTs to fabricate MB-MWNTs/GCE caused a remarkably decrease of the semicircle portion at higher frequencies to form a nearly straight line (Fig. 4b*b*). This may be demonstrated that MB-MWNTs film introduced an advantage to the interfacial electron transfer. Because of the positive charge of MB in the film, the $[Fe(CN)_6]^{4-/3-}$ probe could arrive to the surface of the electrode promptly. The impedance changes of the different modified electrodes revealed that MB had adsorbed on the MWNTs.

Characteristic of the MB-MWNTs/GCE

SEM can effectively prove the surface morphologies of the modified electrode. Figure 5 displayed the characterization of the MB-MWNTs composite film on the GCE by using SEM method. It was obviously demonstrated that the MB-MWNTs composite film was uniformly coated on the electrode surface and formed a network-like structure. The special surface morphology offered a much larger real surface area than the apparent geometric area.
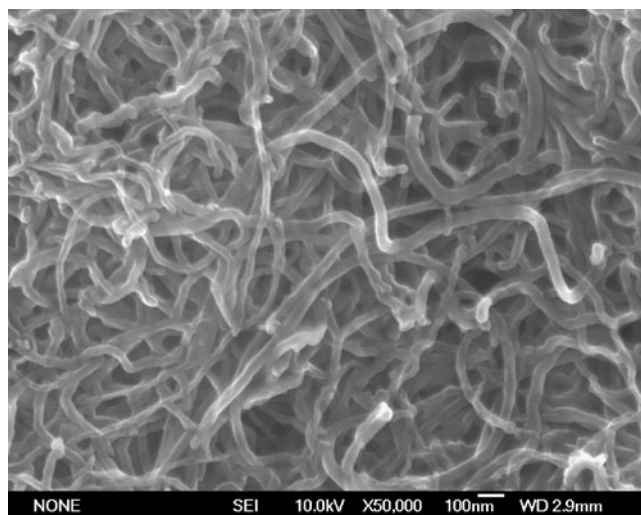
Electrochemical response of DA and UA on MB-MWNTs/GCE

Figure 6a demonstrated the cyclic voltammetry (CV) curves of a mixture of 3.0×10^{-4} M DA and 6.0×10^{-4} M UA (a), 3.0×10^{-4} M DA (b), 6.0×10^{-4} M UA (c), and buffer solution without DA and UA (d) in 0.1 M phosphate solution (pH 3.0) at MB-MWNTs/GCE, respectively. Figure 6a*a* showed two anodic peaks at around the potential of 429 and 603 mV, which attributed to the oxidation of DA and UA with a 174 mV separation of both peaks, which
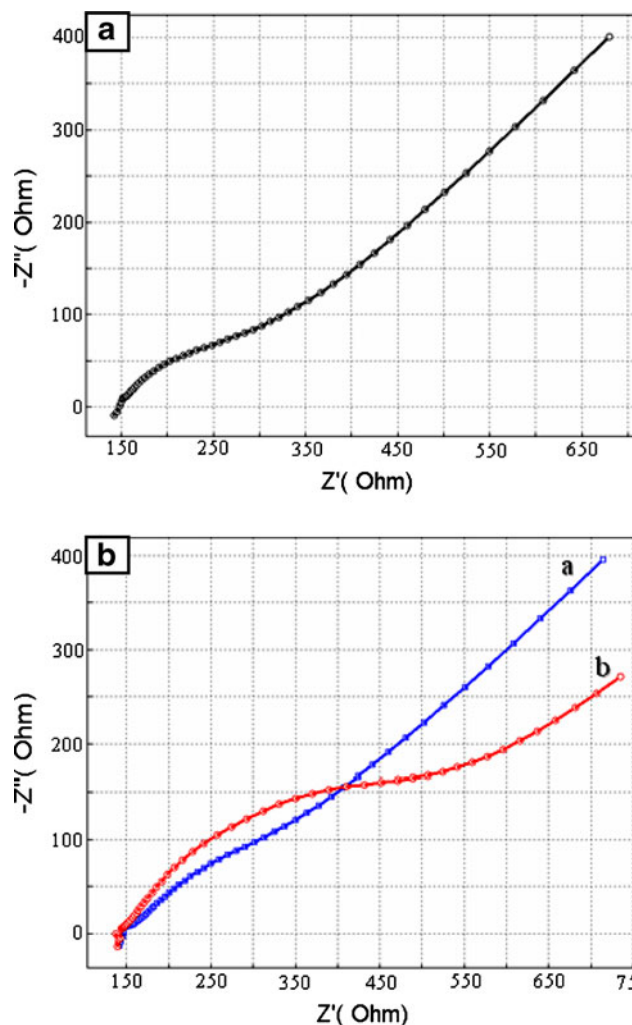
Fig. 4 a Nyquist diagram of EIS at bare GCE; **b** Nyquist diagrams of EIS at MB-MWNTs/GCE (*a*) and MWNTs/GCE (*b*). EIS condition: frequency range: 100 kHz–1 Hz; signal amplitude: 5 mV; solution: 1.0 mM $Fe(CN)_6^{3-/4-}$ in 0.1 M KCl

was broad enough for their simultaneous electrochemical determination of DA and UA. Figure 6b revealed CV responses of a mixture of 3.0×10^{-4} M DA and 6.0×10^{-4} M UA in 0.1 M phosphate solution (pH 3.0) at MB-MWNTs/GCE (a), MWNTs/GCE (b), bare GCE (c) and MB/GCE (d). Under the same conditions, poor anodic peaks of DA and UA were observed at the bare GCE. At the MB/GCE, DA and UA exhibited an overlapped and broad anodic peak extended over a potential region of 450–630 mV with the mixed potential at 530 mV. CV for MWNTs/GCE showed two anodic peaks with a separation of about 144 mV toward DA and UA. Comparing MB-MWNTs/GCE with MWNTs/GCE, a remarkable increase in redox peak currents of DA was observed with the anodic potential shift negatively (more than 30 mV), which revealed that

MB in the matrix of MWNTs/GCE can act as an efficient electron mediator for the electrocatalytic oxidation of DA, besides MWNTs can enhance the electron transfer rate and make more DA participate in the electrochemical reaction due to their accumulation and catalytic ability. The anodic (E_{pa}) and cathodic peak potentials (E_{pc}) of DA were at about 429 and 336 mV (vs. SCE), respectively, and the peak currents ratio of i_{pa}/i_{pc} was about 1.0, which showed that the electrode reaction of DA was almost reversible.

Effect of scanning rate

The effect of scan rate (in the range of 40–300 mV/s) on the peak currents and peak potentials at the MB-MWNTs/GCE in 0.1 M phosphate solution (pH 3.0) containing DA and UA was investigated by CV. As shown in Fig. 7, the anodic peak potentials of DA (E_{DA}) and UA (E_{UA}) at the MB-MWNTs/GCE shifted positively with the increasing of the scan rate. The anodic peak currents of DA (i_{DA}) were found to be directly proportional to the scan rate (v; see Fig. 8), indicating a adsorbed-control oxidation processes occurring at the MB-MWNTs modified GCE. The anodic peak currents of UA (i_{UA}) were found to be directly proportional to the square root of the scan rate ($v^{1/2}$; see Fig. 8, inset), indicating a diffusion-controlled oxidation processes occurring at the MB-MWNTs-modified GCE. The transport characteristics of DA and UA were in good agreement with the previous report on the DNA/poly(p-aminobenzensulfonic acid) bilayer modified electrode [6].

Effect of buffer solution pH

As shown in Fig. 9, the effect of pH on electrochemical reactions of DA and UA at the MB-MWNTs/GCE was also
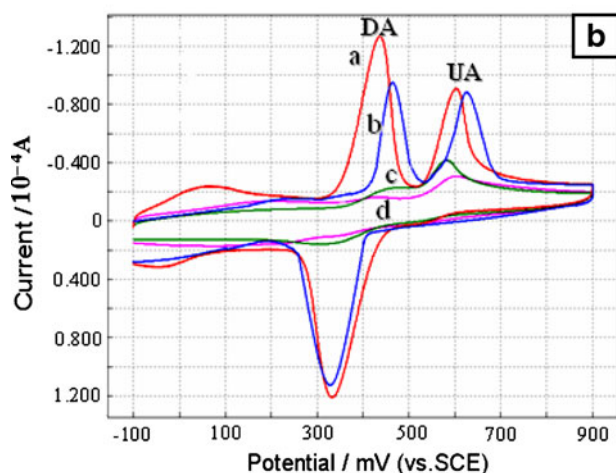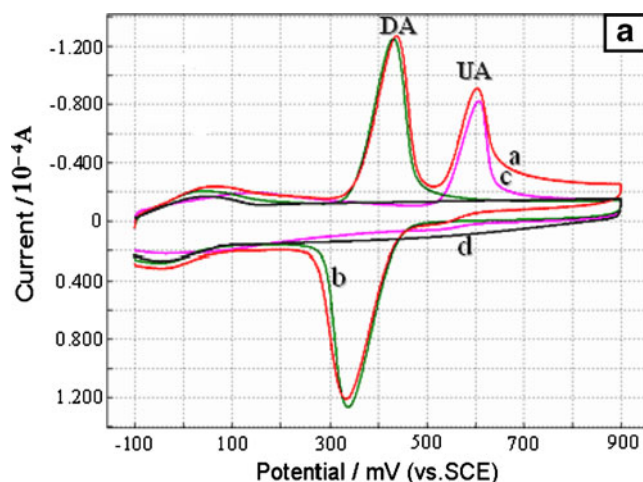
Fig. 6 a CV curves of the mixture containing 3.0×10^{-4} M DA and 6.0×10^{-4} M UA (*a*), 3×10^{-4} M DA (*b*), 6×10^{-4} M UA (*c*), and buffer solution without DA and UA (*d*) in 0.1 M phosphate solution (pH 3.0) at the MB-MWNTs/GCE. b CV curves of the mixture containing 3.0×10^{-4} M DA and 6.0×10^{-4} M UA in 0.1 M phosphate solution (pH 3.0) at different modified electrodes: MB-MWNTs/GCE (*a*), MWNTs/GCE (*b*), bare GCE (*c*), and MB/GCE (*d*); scan rate 80 mV/s

investigated. With pH changing from 3.0 to 8.0, the anodic peak potentials of DA and UA shifted toward more negative potentials. When pH was 3.0, the maximum peak currents of i_{DA} and i_{UA} were achieved with a maximum separation of both anodic peaks, suggesting that pH 3.0 should be selected as the optimum value for the simultaneous determination of DA and UA.
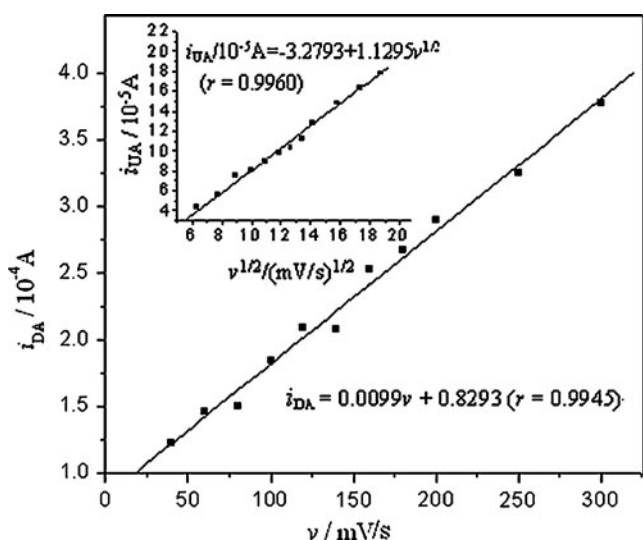
Interferences

For investigating the selectivity of the modified glassy carbon electrode for simultaneous determination of DA and UA,
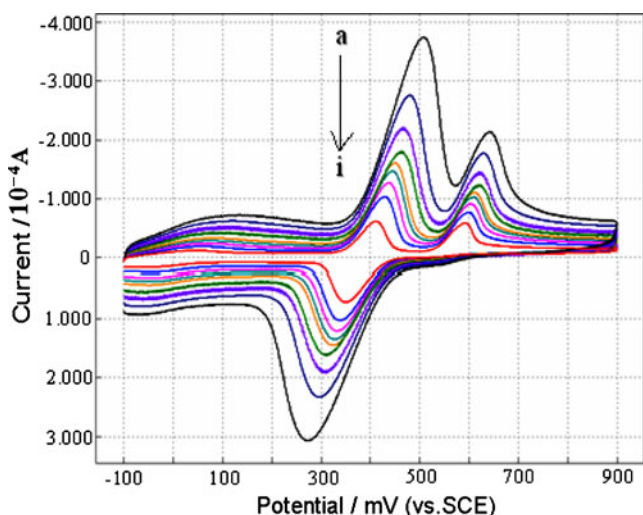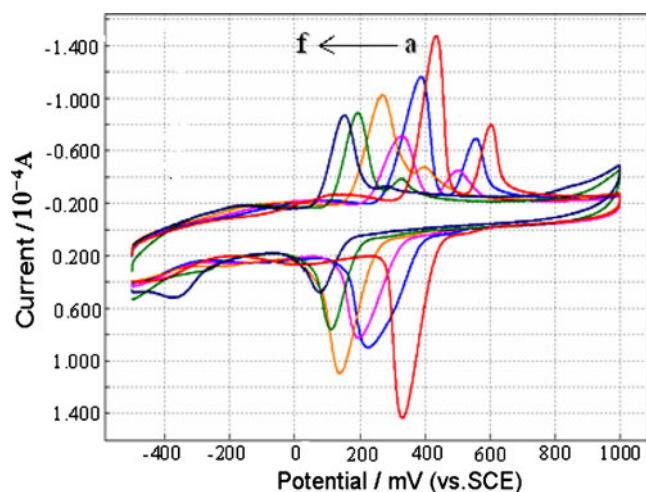
Fig. 7 CV curves of the mixture containing 3.0×10^{-4} M DA and 6.0×10^{-4} M UA at the MB-MWNTs/GCE at different scan rate ($a \rightarrow i$): 300, 250, 200, 160, 120, 100, 80, 60, and 40 mV/s in 0.1 M phosphate solution (pH 3.0)

Fig. 9 CV curves of the mixture containing 3.0×10^{-4} M DA and 3.0×10^{-4} M UA in 0.1 M phosphate buffer at different pH ($a \rightarrow f$): 3.0, 4.0, 5.0, 6.0, 7.0, 8.0; scan rate 80 mV/s

several potential coexistent interference compounds were selected. The tolerance limit ($C_{species}/C_{DA}$) was defined as the maximum concentration of the interfering substance that caused an error less than 10% for the determination of 3.0×10^{-4} M DA in the presence of 6.0×10^{-4} M UA. The following times did not show interference: KCl, MgCl$_2$, glucose, glycine, and CaCl$_2$, 100 times; and CuCl$_2$, five times.

Generally, as the electroactive substance, AA always coexists with DA and UA. The oxidation peak potential of AA is very close to that of DA and UA, which results in poor selectivity determination of DA or UA in real samples on conventional electrodes. Therefore, it is essential to exploit more sensitive, selective, and simple methods for the

segregative determination of AA, DA, and UA. Figure 10 demonstrated the DPASV curves of the mixture of 3.0×10^{-4} M DA and 6.0×10^{-4} M UA (a); 3.0×10^{-3} M AA, 3.0×10^{-4} M DA, and 6.0×10^{-4} M UA (b); 1.0×10^{-3} M AA, 3.0×10^{-4} M DA, and 6.0×10^{-4} M UA (c); 1.0×10^{-3} M AA (d); and 0.1 M phosphate buffer solution (pH 3.0) (e) in 0.1 M phosphate buffer solution (pH 3.0) on MB-MWNTs/GCE. Figure 10d showed an anodic peak at around 200 mV, which was attributed to the oxidation of AA, the separation

Fig. 8 The plot of anodic peak currents of DA vs. the scan rate (v). *Insert*: i_{UA} vs. $v^{1/2}$
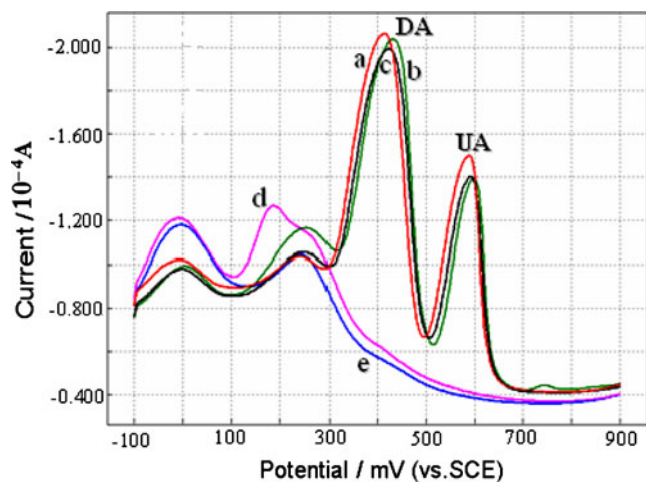
Fig. 10 Differential pulse anodic stripping voltammograms of the mixed solution of 3.0×10^{-4} M DA and 6.0×10^{-4} M UA (*a*), 3.0×10^{-3} M AA, 3.0×10^{-4} M DA and 6.0×10^{-4} M UA (*b*), 1.0×10^{-3} M AA, 3.0×10^{-4} M DA and 6.0×10^{-4} M UA (*c*), 1.0×10^{-3} M AA (*d*) and 0.1 M phosphate buffer solution (pH 3.0; *e*) on the MB-MWNTs/GCE. Instrument parameters: accumulation time 40 s, accumulation potential 100 mV, pulse amplitude 50 mV, pulse increment 4 mV, pulse width 40 ms and pulse period 120 ms
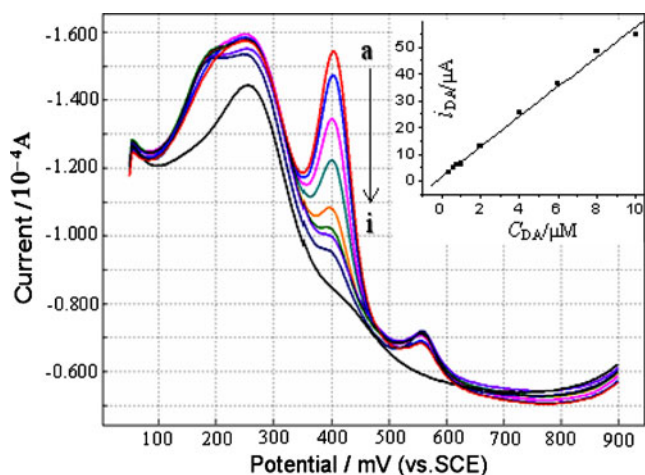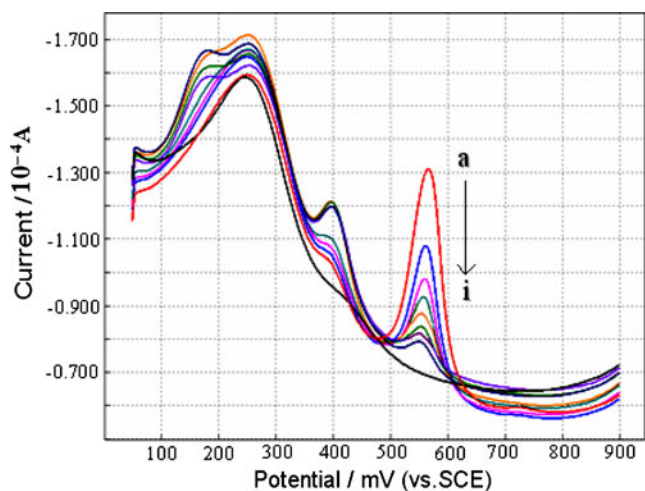
Fig. 11 Differential pulse anodic stripping voltammograms of MB-MWNTs/GCE in 0.1 M phosphate buffer solution (pH 3.0) containing 10.0 μM UA and 1.0×10^{-3} M AA with different concentrations of DA ($a \rightarrow i$): 10.0, 8.0, 6.0, 4.0, 2.0, 1.0, 0.8, 0.6 μM, buffer solution without AA, DA and UA. *Inset*: Plot of anodic peak current of DA vs. DA concentration; other conditions as in Fig. 10

potential of AA and DA was about 219 mV, indicating broad enough separation to eliminate the interference of AA and realize the simultaneous electrochemical determinations of DA and UA in the mixed solution.

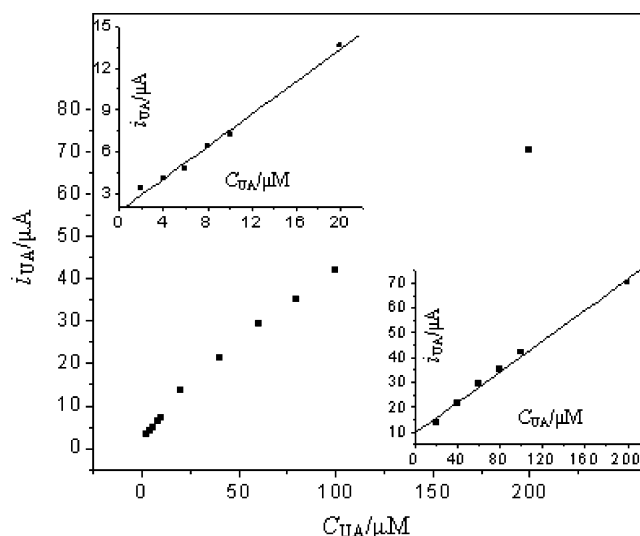Simultaneous determination of DA and UA using DPASV

DPASV was used for the simultaneous determination of DA and UA at the MB-MWNTs/GCE by reason of its

higher current sensitivity and better resolution than CV. The determination of DA and UA in their mixtures in the presence of 1.0×10^{-3} M AA was performed at the MB-MWNTs/GCE when the concentration of one species changed, whereas the other species maintained constant. Figure 11 displayed the DPASV curves of different concentration DA at the MB-MWNTs/GCE containing 10.0 μM UA and 1.0×10^{-3} M AA. The results demonstrated that the anodic peak current (i_{DA}) was linear to the concentration of DA in the range of 0.4–10.0 μM (see Fig. 11, inset), and the linear equation is as follows: $i_{DA}/\mu A = 5.5959 C_{DA}/\mu M + 1.6531$ ($r=0.9972$). The lowest detection limit was 2.0×10^{-7} M.

As shown in Fig. 12, a similar experiment was carried out to determine UA in the presence of 1.0 μM DA and 1.0×10^{-3} M AA, the anodic peak current (i_{UA}) was linear with the concentration of UA in the range of 2.0–20.0 and 20.0–200.0 μM (see Fig. 13). The regression equations are: $i_{UA}/\mu A = 0.5827 C_{UA}/\mu M + 1.7191$ ($r=0.9962$) for the range of 2.0–20.0 μM and $i_{UA}/\mu A = 0.3101 C_{UA}/\mu M + 9.4662$ ($r=0.9972$) for the range of 20.0–200.0 μM. The lowest detection limit was 1.0 μM. Determined parameters of this sensor compared with other modified electrodes based on MWNTs used in the electrocatalysis of DA and UA were represented in Table 1. Compared with the existing reports about simultaneous determination of DA and UA, the proposed method is much more convenient to prepare the MB-MWNTs/GCE-modified electrode. The MB-MWNTs/GCE possesses excellent performances such as simple preparation, high sensitivity, wide linear range, and low detection limits.

Fig. 12 Differential pulse anodic stripping voltammograms of MB-MWNTs/GCE in 0.1 M phosphate buffer solution (pH 3.0) containing 2.0 μM DA and 1.0×10^{-3} M AA with different concentrations of UA ($a \rightarrow i$): 200.0, 100.0, 60.0, 40.0, 20.0, 8.0, 6.0, 4.0 μM, buffer solution without AA, DA and UA

Fig. 13 The relationship between the peak current and concentration of UA in the presence of 1.0 μM DA and 1.0×10^{-3} M AA. *Insets* are the i_{UA} vs. C_{UA} in the range of 2.0–20.0 and 20.0–200.0 μM

Table 1 Comparison of major characteristics of some modified electrodes based on MWNTs used for the DA and uric acid sensing process

Electrode	pH	Method	Analyte	Linear range (μM)	LOD (μM)	Sensitivity (μA μM^{-1})
GCE/CNT-AgHCFNPs [32]	2.0	CV	DA	2.4–130	0.14	Not reported
			UA	2.0–150	0.06	
f-MWCNTs-PNR/GCE [33]	4.0	DPV	DA	75–200	Not reported	0.146
			UA	75–200		0.084
EBNBHCNPE [34]	7.0	DPV	DA	0.1–900	0.087	0.1375
			UA	20–650	15	0.0273
PAA-MWNTs/GCE [5]	7.4	LSW	DA	0.04–3	0.02	Not reported
			UA	0.3–10	0.11	
This work	3.0	DPV	DA	0.4–10	0.2	5.5959
			UA	2.0–200	1.0	0.3101

The repeatability and stability of the MB-MWNTs/GCE

The repeatability and stability are the vital characteristics for the modified electrode, which should be investigated for analytical determination. The same MB-MWNTs/GCE was used for five times successive measurement, and the relative standard deviation (RSD) of the peak current was 3.5% for 3.0×10^{-4} M DA and 4.0% for 6.0×10^{-4} M UA. In addition, five freshly prepared MB-MWNTs/GCE were used to measure 3.0×10^{-4} M DA in the same condition. All five electrodes exhibited similar current responses, and a RSD of 5.6% was obtained. These findings revealed that the electrochemical behavior of the MB-MWNTs/GCE was highly repeatable. The stability of the MB-MWNTs/GCE was studied by determining the steady-state response current of 3.0×10^{-4} M DA every day after preparation, the RSD of steady-state response current was 6.5%. When not in use, the sensor was stored in 0.1 M PBS buffer (pH 7.0) at 4°C. The results showed that the steady-state response current only decreased by 12% after 7 days, indicating that the MB-MWNTs/GCE electrode was considerably stable.

Real samples analysis

In order to fit into the linear range of the method, urine sample and DA hydrochloride injection for detection were accurately diluted with the supporting electrolyte. The detected results were shown in Table 2. The total value of DA in DA hydrochloride injection was 10.48 mg/ml, which was obtained by multiplying the detected value and the diluted factor. The total value of DA was in agreement with the declared content (i.e., 10.0 mg/ml). The total UA concentrations detected in urine sample was 4.54×10^{-3} M, which was consistent with the containing level of a healthy human. In order to test the correctness of the results, standard addition method was used to determine the DA (or UA) sample spiked with suitable DA (or UA). The experimental results were also displayed in Table 2. The results demonstrated that the proposed methods could be efficiently used for the determination of DA and UA.

Conclusions

The MB-MWNTs/GCE displayed good electrocatalytic activity for the oxidation of DA and UA. In addition, the modified electrode exhibited higher selectivity in electro-analysis of DA and UA in their mixture solution with a 174 mV separation of their oxidation peaks, showing that MB-MWNTs/GCE has the ability for the simultaneous determination of DA and UA. The coexisting substance of AA declared no interference to the simultaneous determination of DA and UA. The proposed method was used to

Table 2 Results of the determination of DA and UA in real samples containing 1.0×10^{-3} M AA (n=5)

Sample	Species	Species added (μM)	Proposed method (μM)	Recovery (%)	RSD (%)
DA hydrochloride injection	DA	–	5.52	–	2.6
	DA	2.0	1.9	95.0	3.1
	DA	6.0	5.8	96.6	2.8
Urine	UA	–	45.4	–	3.0
	UA	20.0	20.1	100.9	2.0
	UA	60.0	58.6	97.7	3.2

the determination of DA and UA in real samples with satisfactory results.

References

1. Wightman RM, May LJ, Michael AC (1988) Anal Chem 60:769A
2. Liu A, Honma I, Zhou HS (2005) Biosens Bioelectron 21:809
3. Mo JW, Ogorevc B (2001) Anal Chem 73:1196
4. Zen JM, Jou JJ, Ilangovan G (1998) Analyst 123:1345
5. Liu AH, Honma I, Zhou HS (2007) Biosens Bioelectron 23:74
6. Lin XQ, Kang GF, Lu LP (2007) Bioelectrochemistry 70:235
7. Kang GF, Lin XQ (2006) Electroanalysis 18:2458
8. Zhang YZ, Pan Y, Su S, Zhang LP, Li SP, Shao MW (2007) Electroanalysis 19:1695
9. Wang GF, Sun JG, Zhang W, Jiao SF, Fang B (2009) Microchim Acta 16:4357
10. Zhu SY, Li HJ, Niu WX, Xua GB (2009) Biosens Bioelectron 25:940
11. Yao H, Sun YY, Lin XH, Tang YH, Huang LY (2007) Electrochim Acta 52:6165
12. Kalimuthu P, John SA (2009) Bioelectrochem 77:13
13. Ensafi AA, Khayamian MTT (2009) J Electroanal Chem 633:212
14. Zhang R, Jin GD, Chen D, Hu XY (2009) Sens Actuators B 138:174
15. Li YX, Lin XQ (2006) Sens Actuators B 115:134
16. Zare HR, Rajabzadeh N, Nasirizadeh N, Ardakani MM (2006) J Electroanal Chem 589:60
17. Zheng D, Ye JS, Zhou L, Zhang Y, Yu CZ (2009) J Electroanal Chem 625:82
18. Cao XM, Xu YH, Luo LQ, Ding YP, Zhang Y (2010) J Solid State Electrochem 14:829
19. Iijima S (1991) Nature 354:56
20. Ajayan PM (1999) Chem Rev 99:1787
21. Yao H, Li N, Xu S, Xu JZ, Zhu JJ, Chen HY (2005) Biosens Bioelectron 21:372
22. Liu CY, Hu JF, Hu JM, Tanga HW (2006) Electroanalysis 18:478
23. Xian YZ, Liu F, Xian Y, Zhou YY, Jin LT (2006) Electrochim Acta 51:6527
24. Xiao MW, Wang LS, Wu YD, Huang XJ, Dang Z (2008) J Solid State Electrochem 12:1159
25. Yan YM, Zhang MN, Gong KP, Su L, Guo ZX, Mao LQ (2005) Chem Mater 17:3463
26. Yogeswaran U, Chen SM (2008) Sens Actuators B 130:739
27. Li Q, Zhang J, Yan H, He M, Liu Z (2004) Carbon 42:287
28. Zhang J, Lee JK, Wu Y, Murray RW (2003) Nano Lett 3:403
29. Zhang M, Gong K, Zhang H, Mao L (2005) Biosens Bioelectron 20:1270
30. Chen RJ, Zhang Y, Wang D, Dai H (2001) J Am Chem Soc 123:3838
31. Sagara T, Niki K (1993) Langmuir 9:831
32. Mozhgan KM, Aboozar T (2010) Talanta 80:1657
33. Yogeswaran U, Chen SM (2007) Electrochim Acta 52:5985
34. Mohammad MA, Hadi B, Bahram G, Hossein N, Maryam N (2009) Bioelectrochemistry 75:1